arXiv:1302.2196v1 [hep-ph] 9 Feb 2013

RBRC-1005

Phase structure and Hosotani mechanism in gauge theories with compact dimensions revisited

Kouji Kashiwa*
RIKEN/BNL, Brookhaven National Laboratory, Upton, NY 11973

Tatsuhiro Misumi†
Department of Physics, Brookhaven National Laboratory, Upton, NY 11973

Abstract

We investigate the phase structure of $SU(3)$ gauge theory in four and five dimensions with one compact dimension by using perturbative one-loop and PNJL-model-based effective potentials, with emphasis on spontaneous gauge symmetry breaking. When adjoint matter with the periodic boundary condition is introduced, we have rich phase structure in the quark-mass and compact-size space with gauge-symmetry-broken phases, called the $SU(2)\times U(1)$ split and the $U(1)\times U(1)$ re-confined phases. Our result is qualitatively consistent with the recent lattice calculations. When fundamental quarks are introduced in addition to adjoint quarks, the split phase becomes more dominant and larger as a result of explicit center symmetry breaking. We also show that another $U(1)\times U(1)$ phase (pseudo-reconfined phase) with negative vacuum expectation value of Polyakov loop exists in this case. We study chiral properties in these theories and show that chiral condensate gradually decreases and chiral symmetry is slowly restored as the size of the compact dimension is decreased.

---

*kashiwa@ribf.riken.jp
†tmisumi@bnl.gov

I. INTRODUCTION

Now that the Higgs-like particle has been discovered in Large Hadron Collider (LHC) [1, 2], one of primary interests of particle physics is to understand mechanism of dynamical electroweak symmetry breaking. To settle down the unsolved issues including the hierarchy problem, there have been proposed several promising courses including supersymmetric, composite-Higgs and extra-dimensional models. Among them, the gauge-Higgs unification with extra dimensions [3, 4] produces brilliant dynamics of gauge symmetry breaking, called the Hosotani mechanism [4–10], with the Higgs particle as an extra-dimensional component of the gauge field: when adjoint fermions are introduced with periodic boundary condition (PBC) in gauge theory with a compact dimension, the compact-space component of the gauge field can develop a non-zero vacuum expectation value (VEV), which breaks the gauge symmetry to its subgroup spontaneously. This phenomenon originates in the non-abelian Aharonov-Bohm effect. There have been proposed a number of BSM models directly and indirectly based on this mechanism [11–23]

Recently, the same phenomenon has been observed in a different context. As well-known, the imaginary time dimension is compacted in the finite-temperature (Quantum Chromodynamics) QCD. When the adjoint fermion is introduced with PBC in the theory, it was shown that exotic phases appear [24–29], where the color trace of Polyakov line takes non-trivial VEV leading to the dynamical gauge symmetry breaking. This can be interpreted as $R^3 \times S^1$ realization of the Hosotani mechanism. Further study is now required to understand detailed properties and phase diagram for this case. As for the five-dimensional gauge theory on $R^4 \times S^1$, lattice simulation is still at the stage to understand the nature of 5D pure Yang-Mills theory. First attempt was done in Ref. [30] and recent progress was shown in Ref. [31–53]. At the present, we have no detailed investigation on the phase structure of the five-dimensional gauge theory with dynamical quarks.

The purpose of our work is to understand properties of gauge theories with quarks on $R^3 \times S^1$ and $R^4 \times S^1$ by using effective theories and show a guideline for further lattice simulations. We focus on the phase structure in $SU(3)$ gauge theory by mainly using the perturbative one-loop effective potential. When we look into chiral properties, the Polyakov-loop-extended Nambu–Jona-Lasinio (PNJL) model [54–57] is introduced. We obtain the phase diagram in the quark-mass and compacted-size space for several different choices of fermion representations and boundary conditions. In the theory with adjoint fermions with PBC, we find rich phase diagram with unusual phases where $SU(3)$ gauge symmetry is spontaneously broken to $SU(2) \times U(1)$ (split phase) or $U(1) \times U(1)$ (re-confined phase). This result is consistent with the recent lattice simulations [25, 29] and the perturbative calculations for massless quarks [9, 10]. We show that chiral condensate is gradually decreased and the chiral symmetry is slowly restored with the compacted size being decreased although small chiral transitions coincide with the deconfined/split and split/reconfined transitions. We also study phase diagram for the case with both fundamental and adjoint quarks, and show that the split phase becomes more dominant as a result of the explicit breaking of Z_3 center symmetry. This result indicates that the $SU(3) \to SU(2) \times U(1)$ phase, which is of significance in terms of phenomenology, can be controlled by adjusting the number of fundamental flavors. In this case we point out that another unusual ($U(1) \times U(1)$) phase with negative VEV of color-traced Polyakov loop emerges, which we call "pseudo-reconfined phase".

We note similar investigation on the phase diagram of compact-space gauge theory with PBC fermions were shown in [24, 26, 28], where the authors focus on the volume independence of the vacuum structure from the viewpoint of the large N reduction [59–66]. In order to reproduce the confined phase at low temperature, they used the gluon effective potentials with the mass-dimension parameter, which leads to explicit gauge symmetry breaking. Since these effective potentials do not suit our purpose of studying spontaneous gauge symmetry breaking due to the Hosotani mechanism, we mainly use setups with manifest gauge symmetry.

This paper is organized as following. In Sec. II, we show our setups including the one-loop potential and the PNJL model. Sec. III shows our numerical results for four dimensional cases. Sec. IV we show the results for five-dimensional cases. Sec. V is devoted to summary.

II. EFFECTIVE POTENTIAL

In this section we discuss our setups for SU(N) gauge theory. The one-loop effective potential is composed of two parts, gluonic and quark contributions. Since our goal is to study the phase diagram in terms of Wilson-line phases (Polyakov-line phases), q_i ($i = 1, 2, ..., N$), we will write the effective potential as a function of these variables. Besides the one-loop potential, we consider the contribution from the chiral part, which originates in the NJL-type four-point interactions. The total effective potential is then regarded as that of the PNJL model [55] as a function of the q_i and the chiral condensate σ. Depending on our purposes, we in some cases use only the perturbative one-loop effective potential, and in other cases use the PNJL effective potential. We also comment on possible deformation reflecting non-perturbative effects in the gluonic contribution.

A. SU(N) in four dimensions

We begin with one-loop effective potential for $SU(N)$ gauge theory. In four dimensions, the finite-tempreature one-loop effective potential for gauge bosons and fermions is well studied in Ref. [67, 68]. What we do in the present study is just to regard the compacted imaginary-time direction as one of the spatial direction, and to replace T by $1/L$ where L is a size of the compacted dimension.

Firstly, we rewrite the $SU(N)$ gauge boson field as

$$A_\mu = \langle A_y \rangle + \tilde{A}_\mu, \tag{1}$$

where y stands for a compact direction and $\langle A_y \rangle$ is a vacuum expectation value (VEV) while $\tilde{A}_\mu$ is fluctuation from it. The VEV can be replaced by

$$\langle A_y \rangle = \frac{2\pi}{gL} q, \tag{2}$$

where q's color structure is $\mathrm{diag}(q_1, q_2, ..., q_N)$ with $q_1 + q_2 + \cdots + q_{N-1} + q_N = 0$ and each component is determined as $(q_i)_{mod\ 1}$. We note that eigenvalues of q_i are invariant under all gauge transformations preserving boundary conditions. Then we can easily observe spontaneous gauge symmetry breaking from values of q_i in the vacuum. For detailed argument on gauge transformation for this topic, see [9] for example. The gluon one-loop effective potential $\mathcal{V}_g$ is expressed as

$$\mathcal{V}_g = -\frac{2}{L^4\pi^2} \sum_{i,j=1}^{N} \sum_{n=1}^{\infty} \Big(1 - \frac{1}{N}\delta_{ij}\Big) \frac{\cos(2n\pi q^{ij})}{n^4} \tag{3}$$

where $q_{ij} = (q_i - q_j)_{mod\ 1}$ and N is the number of color degrees of freedom.

The contribution from massless fundamental quarks $\mathcal{V}_f$ is given by

$$\mathcal{V}_f = \frac{4N_f}{L^4\pi^2} \sum_{i=1}^{N} \sum_{n=1}^{\infty} \frac{\cos[2\pi n(q_i + 1/2)]}{n^4}, \tag{4}$$

where N_f is the number of fundamental flavors. Depending on boundary conditions, we should replace $q_i + 1/2$ by $q_i + \phi$. For example, the choice of $\phi = 0$ describes quarks with periodic boundary conditions. From here, we denote $\mathcal{V}_f^{\phi}$ as effective potential of the fundamental fermion with boundary angle ϕ. The contribution from massive fundamental quarks is expressed by using the second kind of the modified Bessel function $K_2(x)$ as

$$\mathcal{V}_f^{\phi}(N_f, m_f) = \frac{2N_f m_f^2}{\pi^2 L^2} \sum_{i=1}^{N} \sum_{n=1}^{\infty} \frac{K_2(n m_f L)}{n^2} \cos[2\pi n(q_i + \phi)], \tag{5}$$

where m_f is the fundamental fermion mass. (We assume the same mass for all flavors.) Here the second kind of the modified Bessel function $K_\nu(x)$ is defined as

$$K_\nu(x) = \frac{\sqrt{\pi}(x/2)^\nu}{\Gamma(\nu + 1/2)} \int_1^\infty e^{-xt}(t^2 - 1)^{\nu - \frac{1}{2}} dt, \tag{6}$$

where $\Gamma(x)$ is the gamma function. The adjoint quark contribution $\mathcal{V}_a^{\phi}$ can be easily obtained by the following replacement,

$$\mathcal{V}_a^{\phi}(N_a, m_a) = \frac{2N_a m_a^2}{\pi^2 L^2} \sum_{i,j=1}^{N} \sum_{n=1}^{\infty} \left(1 - \frac{1}{N}\delta_{ij}\right) \frac{K_2(n m_a L)}{n^2} \cos[2\pi n(q_{ij} + \phi)], \tag{7}$$

where N_a and m_a are the number of flavors and the mass for adjoint fermions. For the gauge theory with N_f fundamental and N_a adjoint fermions with arbitrary boundary conditions, the total one-loop effective potential is given by

$$\mathcal{V} = \mathcal{V}_g + \mathcal{V}_f^{\phi}(N_f, m_f) + \mathcal{V}_a^{\phi}(N_a, m_a). \tag{8}$$

Now we consider contribution from the chiral sector. We introduce the four-point interaction at the action level as

$$g_S[(\bar{\psi}\psi)^2 + (\bar{\psi} i\gamma_5 \vec{\tau}\psi)^2], \tag{9}$$

where ψ is a two-flavor fermion field and g_S is the effective coupling constant with the mass dimension minus two. (We here concentrate on the two-flavor case.) By introducing the auxiliary field σ, we show that introduction of the above term (9) leads to addition of the following zero-temperature contribution to the one-loop effective potential (8) [28],

$$\mathcal{V}_\chi = g_S \sigma^2 - \frac{d_R \Lambda^4}{4\pi^2} \left[\left(2 + \frac{m_c^2}{\Lambda^2}\right) \sqrt{1 + \frac{m_c^2}{\Lambda^2}} + \frac{m_c^4}{\Lambda^4} \log\left(\frac{m_c/\Lambda}{1 + \sqrt{1 + m_c^2/\Lambda^2}} \right) \right], \tag{10}$$

where Λ is a cutoff scale of the effective theory and m_c stands for constituent quark mass $m_c = m - 2g_S\sigma$. Depending on fundamental or adjoint representations, d_R takes N or $N^2 - 1$

respectively. In the case that we consider both fundamental and adjoint quarks, we need two different sets of chiral sectors. The total effective potential combined with the chiral contribution is then given by

$$\mathcal{V}_{\rm total} = \mathcal{V} + \mathcal{V}_{\chi}. \tag{11}$$

This potential is valid for the weak-coupling region because it is basically based on the perturbative calculations, and chiral properties we obtain from it is at least valid for a small L region. We note that the cutoff scale Λ and the effective-coupling g_S should be chosen to reproduce the known results. We note that this total effective potential is identical to that of the PNJL model [55] adopting the one-loop potential as the gluon contribution,

$$\mathcal{L}_{\rm PNJL} = \bar{\psi}(\gamma_\mu D_\mu + m)\psi - g_S[(\bar{\psi}\psi)^2 + (\bar{\psi}i\gamma_5\vec{\tau}\psi)^2] + \mathcal{V}_g, \tag{12}$$

with $D_j = \partial_j$, $D_4 = \partial_4 + iA_4$. We thus call the total effective potential (11) PNJL or PNJL-based effective potential.

We here comment on the PNJL model. In the standard use of the PNJL model, the gluonic contribution $\mathcal{V}_g$ is replaced by the "non-perturbatively"-deformed ones: in order to mimic the confinement/deconfinement phase transition in the study on QCD phase diagram,, the one-loop gluon potential should be replaced by some nonperturbative versions. We have several schemes including the ones adopted in Ref. [27, 28, 69, 70], the one-loop *ansatz* used in Ref. [71] and the strong-coupling lattice potential in Ref. [55, 58]. In all the modifications able to reproduce the phase transition, however, the $SU(N)$ gauge symmetry is explicitly broken due to the mass-dimension parameters. Since the non-perturbative modification does not suit our purpose of classifying the gauge-broken phases, we will mainly adopt one-loop effective potential as the gluonic contribution in our PNJL model and just discuss how the phase diagram is changed by the deformation in the next section.

B. SU(N) in five dimensions

In the five-dimensional case, most of the setup is parallel to the four-dimensional case except for difference of mass dimensions of fields and parameters. We here show the one-loop effective potential of gluon and quarks below. The five-dimensional one-loop effective potential in the gluon sector is given by

$$\mathcal{V}_g = -\frac{9}{4\pi^2 L^5}\sum_{i,j=1}^{N}\sum_{n=1}^{\infty}\Big(1-\frac{1}{N}\delta_{ij}\Big)\frac{\cos(2\pi n q_{ij})}{n^5}, \tag{13}$$

which has $1/L^5$ dimension. The effective potential for massless fermions in this case is given by

$$\begin{aligned}\mathcal{V}_f^{1/2} &= -2T\int\frac{dk}{8\pi^2}k^3\Big[\ln\Big(1+e^{-L|\mathbf{k}|+2i\pi q^{ij}}\Big)+\ln\Big(1+e^{-L|\mathbf{k}|-2i\pi q^{ij}}\Big)\Big]\\ &= \frac{3}{L^5\pi^2}\sum_{n=1}^{\infty}\frac{\cos[2\pi n(q^{ij}+1/2)]}{n^5}.\end{aligned} \tag{14}$$

The effective potential of the massless fundamental and adjoint fermions with arbitrary boundary condition is expressed as

$$\mathcal{V}_f^{\phi} = \frac{3N_f}{\pi^2 L^5}\sum_{i=1}^{N}\sum_{n=1}^{\infty}\frac{\cos[2\pi n(q_i+\phi)]}{n^5}, \tag{15}$$

$$\mathcal{V}_a^{\phi} = \frac{3N_a}{\pi^2 L^5}\sum_{i,j=1}^{N}\sum_{n=1}^{\infty}\Big(1-\frac{1}{N}\delta_{ij}\Big)\frac{\cos[2\pi n(q_{ij}+\phi)]}{n^5}. \tag{16}$$

For the massive fermion, we should replace $|\mathbf{k}|$ by $E_p=\sqrt{\mathbf{p}^2+m^2}$ in Eq. (14). To evaluate the integration, we should expand the logarithm in the same way as the four dimesional case. Individual integration is done by using the Bessel function as

$$\begin{aligned}\frac{e^{\pm 2i\pi n q^{ij}}}{n}\int_0^{\infty}p^3 e^{-nLE_{\rm p}}dp &= -\frac{e^{\pm 2i\pi n q^{ij}}}{n^2}\frac{\partial}{\partial L}\int_1^{\infty}m^3(t^2-1)e^{-nLmt}dt.\\ &= -\frac{e^{\pm 2i\pi n q^{ij}}}{n^2}\frac{2^{3/2}}{\sqrt{\pi}}\frac{\partial}{\partial L}\Big[\Big(\frac{m}{nL}\Big)^{3/2}K_{3/2}(nLm)\Big]\\ &= \frac{e^{\pm 2i\pi n q^{ij}}}{n}\frac{2^{3/2}m}{\sqrt{\pi}}\Big(\frac{m}{nL}\Big)^{3/2}K_{5/2}(nLm).\end{aligned} \tag{17}$$

Then, the potential contributions from massive fermions are obtained by using the $K_{5/2}(x)$ as

$$\mathcal{V}_f^{\phi}(N_f,m_f) = \frac{\sqrt{2}N_f(m_f/L)^{5/2}}{\pi^{5/2}}\sum_{i=1}^{N}\sum_{n=1}^{\infty}\frac{K_{5/2}(nm_fL)}{n^{5/2}}\cos[2\pi n(q_i+\phi)], \tag{18}$$

$$\mathcal{V}_a^{\phi}(N_a,m_a) = \frac{\sqrt{2}N_a(m_a/L)^{5/2}}{\pi^{5/2}}\sum_{i,j=1}^{N}\sum_{n=1}^{\infty}\Big(1-\frac{1}{N}\delta_{ij}\Big)\frac{K_{5/2}(nm_aL)}{n^{5/2}}\cos[2\pi n(q_{ij}+\phi)]. \tag{19}$$

We here comment on treatment of parity pairs. When we need a parity-even mass term in odd dimensions (e.g. Z_2 orbifolded theory), we need a set of parity pairs $\psi^{\pm}(-y)=\pm\psi(y)$

in the action [12]. Although our study does not take much care about such a case, we note that the factor two appears in front of the fermion potentials if the parity pair is introduced. It is thus the same situation as doubled flavors within this setup. In Sec. IV, we will see that the phase diagram changes depending on the choice of the parity pair in five dimensions.

III. PHASE STRUCTURE IN FOUR DIMENSIONS

In this section, we investigate the phase structure in the compacted-size L^{-1} and quark-mass m space for $SU(3)$ gauge theories on $R^3 \times S^1$. Because of the relation $-q_3 = q_1 + q_2$, the vacuum structure is discussed just from the (q_1, q_2) potential. In the following we begin with investigation on vacuum and phase structures based on the one-loop potential (8) for several choices of matters and boundary conditions. We note that we will sometimes consider one-flavor cases as $(N_f, N_a) = (0, 1)$ or $(N_f, N_a) = (1, 1)$. Since the anomaly is not implemented and difference of one- and multiple-flavors just appears as an overall factor in the effective potential, our four-dimensional results are qualitatively unchanged even for the two-flavor cases as $(N_f, N_a) = (0, 2)$ or $(N_f, N_a) = (2, 2)$. Thus, these one-flavor examples are sufficient for our purpose of studying phase diagram qualitatively. (Things are different in five dimensions as shown in Sec. IV.)

In the appendix. A, we summarize the potential minima for gauge-symmetry-preserved cases, which are not our main results. We show the contour plots of the effective potentials for $(N_f, N_a) = (0, 0)$ in Fig. 19, $(N_f, N_a) = (1, 0)$ with the anti-periodic boundary condition (aPBC) in Fig. 20, $(N_f, N_a) = (1, 0)$ with the periodic boundary condition (PBC) in Fig. 21, and $(N_f, N_a) = (0, 1)$ with aPBC in Fig. 22. We set $m_f = m_a = 0$ in these cases. In the pure-gauge and gauge+adjoint theories, the three degenerate vacua clearly reflects the Z_3 center symmetry while the introduction of fundamental fermions lift of the degeneracy, which means breaking of the center symmetry. We note that the global minima are given by any of $(q_1, q_2) = (0, 0), (1/3, 1/3), (-1/3, -1/3)$, and we have $q_1 = q_2 = q_3$ (mod 1) in the vacuum. It obviously shows that the $SU(3)$ symmetry remains in all these cases.

Now, we shall look into the case with spontaneous gauge symmetry breaking. We consider $(N_f, N_a) = (0, 1)$ with PBC. We note that this theory has exact center symmetry, and all the phases, even the gauge-broken phase, should reflect this symmetry. Figure 1 shows the effective potential $[\mathcal{V}_g + \mathcal{V}_a^0]L^4$. The left contour plot is obviously different from the gauge-

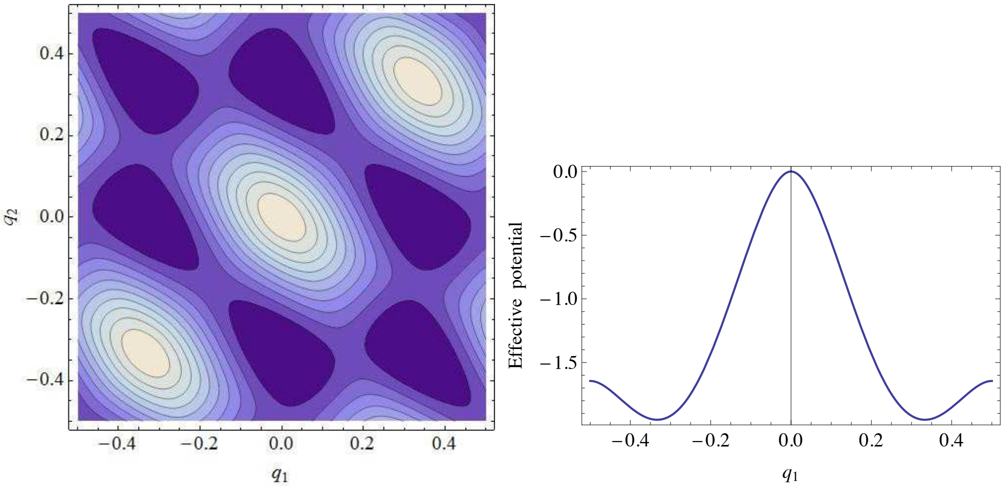

FIG. 1: The one-loop effective potential of $SU(3)$ gauge theory on $R^3 \times S^1$ with one adjoint fermion with PBC $[\mathcal{V}_g + \mathcal{V}_a^0(N_a = 1, m_a = 0)]L^4$. (Right) The contour plot as a function of q_1 and q_2. Thicker region stands for deeper region of the potential. (Left) The effective potential as a function of q_1 with $q_2 = 0$. The global minima are located at $(q_1, q_2) = (\pm 1/3, 0)$.

symmetric cases. Careful search shows that the minima are located at $(q_1, q_2) = (0, 1/3)$, $(1/3, 0)$, $(-1/3, 1/3)$, $(-1/3, 0)$, $(0, -1/3)$, $(1/3, -1/3)$. It means the vacua are given by permutations of $(q_1, q_2, q_3) = (0, 1/3, -1/3)$, and $SU(3)$ gauge symmetry is broken into $U(1) \times U(1)$. This is the famous result, known as the Hosotani mechanism, where the Aharonov-Bohm effect in the compacted dimension nontrivially breaks gauge symmetry [4, 5, 9, 10]. We note that this situation is sometimes called "re-confined phase" [29] since the color fundamental trace of the Polyakov loop $\Phi \equiv \mathrm{Tr}_F\ P$ becomes zero.

To study the phase diagram, we introduce nonzero quark mass. Figure 2 shows the effective potential $[\mathcal{V}_g + \mathcal{V}_a^0(N_a, m_a)]L^4$ as a function of q_1 with $q_2 = 0$ for $mL = 1.2$, 1.6, 2.0 and 3.0 from left to right panels ($m \equiv m_a$). It is clearly seen that there is the first-order phase transition in the vicinity of $mL = 1.6$. This is a transition between the re-confined phase and the other gauge-broken phase, which we call the "split phase" [29]. The contour plots for $mL = 1.6$ and $mL = 1.8$ are shown in Fig. 3. The $mL = 1.8$ case corresponds to the split phase. The global minima in the split phase are given by

- $\mathrm{Im}\ \Phi = 0$: $(q_1, q_2) = (0, 0.5)$, $(0.5, 0.5)$, $(0.5, 0)$,
- $\mathrm{Im}\ \Phi > 0$: $(q_1, q_2) = (1/6, -1/3)$, $(-1/3, 1/6)$, $(1/6, 1/6)$,

- Im $\Phi < 0$: $(q_1, q_2) = (1/3, -1/6)$, $(-1/6, -1/6)$, $(-1/6, 1/3)$.

These results indicate that the vacuum in the first set is given by permutations of $(q_1, q_2, q_3) = (0, 0.5, 0.5)$, and $SU(3)$ gauge symmetry is broken into $SU(2)\times U(1)$. The vacua for other two sets are derived by the Z_3 transformation of $(q_1, q_2, q_3) = (0, 0.5, 0.5)$. From the viewpoint of phenomenological symmetry breaking, this phase and similar phases for large color numbers are the most preferable.

In Fig. 4 we depict the L^{-1}-m phase diagram with one PBC adjoint quark $(N_f, N_a) = (0, 1)$ based on the one-loop effective potential. We note that, as m appears as mL in this one-loop effective potential, we have scaling in the phase diagram and we can choose arbitrary mass-dimension unit. Since we drop the non-perturbative effect in the gluon potential, we have no confined phase at small L^{-1} (at low temperature). The order of the three phases in Fig. 4 (deconfined $SU(3)$ → split $SU(2) \times U(1)$ → reconfined $U(1) \times U(1)$ from small to large L^{-1}.) is consistent with that of the lattice simulation except that we have no confined phase. We note that all the critical lines in the figure are first-order. In Fig. 5 we depict a schematic distribution plot of Φ in the complex plane. It is obvious that each phase reflects Z_3 symmetry. In the split phase, Φ takes nonzero values but in a different manner from the deconfined phase. In the re-confined phase, we exactly have $\Phi = 0$ with the vacuum breaking the gauge symmetry.

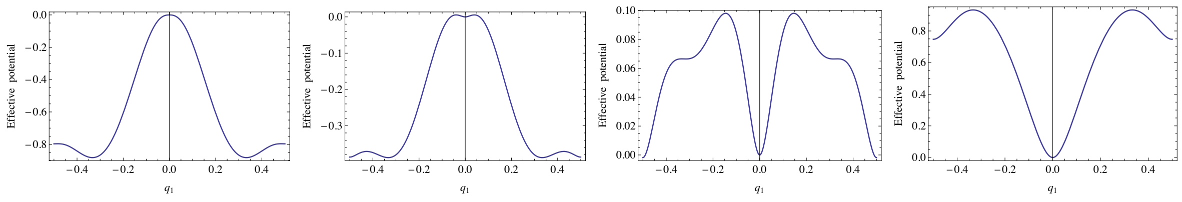

FIG. 2: The one-loop effective potential of $SU(3)$ gauge theory on $R^3 \times S^1$ with one PBC adjoint quark as a function of q_1 with $q_2 = 0$ $[\mathcal{V}_g + \mathcal{V}_a^0]L^4$, for $mL = 1.2$ (reconfined), 1.6 (reconfined↔split), 2.0 (split↔deconfined) and 3.0 (deconfined).

We next turn on the chiral sector and consider the PNJL effective potential (11). We investigate chiral properties of $(N_f, N_a) = (0, 2)$ $SU(3)$ gauge theory on $R^3 \times S^1$. [79]. Before proceeding to the main topic, we discuss validity of the effective model (11) for the purpose of studying chiral properties at weak-coupling region. Although we have no confined phase nor confined/deconfined phase transition in our model, the chiral restoration

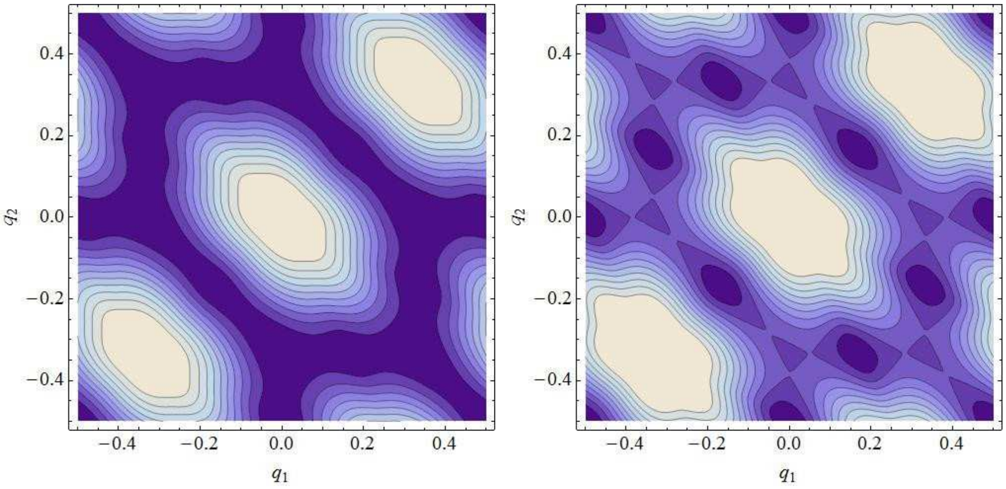

FIG. 3: Contour plot of the one-loop effective potential of $SU(3)$ gauge theory on $R^3 \times S^1$ with one PBC adjoint quark $[(\mathcal{V}_g)_{pert} + \mathcal{V}_a^0]L^4$, for $mL = 1.6$ and 1.8 ($SU(2) \times U(1)$ split phase) as a function of q_1 and q_2. Thicker region indicates deeper region of the potential.

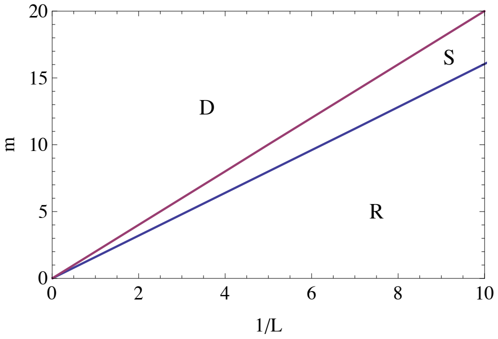

FIG. 4: L^{-1}-m phase diagram for $SU(3)$ gauge theory on $R^3 \times S^1$ with one PBC adjoint quark based on one-loop effective potential. D stands for "deconfined ($SU(3)$)", S for "split ($SU(2) \times U(1)$)" and R for "re-confined ($U(1) \times U(1)$)" phases. Phase transitions are first-order.

associated with the phase transition is correctly reproduced in this model for the known cases: $(N_f, N_a) = (2, 0)$ with aPBC, $(N_f, N_a) = (2, 0)$ with PBC and $(N_f, N_a) = (0, 2)$ with aPBC. We depict behavior of the constituent mass for these cases in Fig. 6, where the chiral phase transition takes place at some point for the three cases. The parameters are chosen so as to have the correct critical temperatures in finite-temperature $SU(3)$ gauge theory with aPBC quarks [72, 73], $\Lambda = 0.63$ GeV and $g_S\Lambda^2 = 2.19$ for fundamental quarks and $\Lambda = 23.22$ GeV and $g_S\Lambda^2 = 0.63$ for adjoint quarks [28].

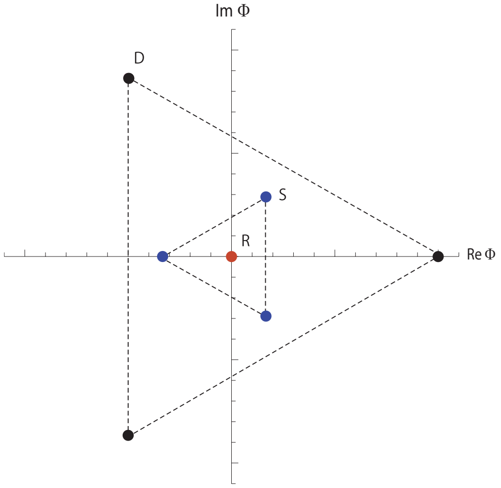

FIG. 5: Schematic distribution plot of Polyakov loop Φ as a function of Re Φ and Im Φ for $SU(3)$ gauge theory on $R^3 \times S^1$ with one PBC adjoint quark.

We are now convinced that the model can work to study chiral properties, and we go on to the main topic, $(N_f, N_a) = (0, 2)$ with PBC. We calculate the PNJL effective potential in Eq. (11) and search for the vacua for q_1, q_2 and σ. We depict the phase diagram for this case in Fig. 7. Due to nonzero constituent mass, the whole phase diagram is shifted, and we have phase transitions even for a $m_a = 0$ massless case. We also note that the critical lines are curved due to the dimensionful parameters introduced. Although our analysis is valid only for the weak-coupling regime, the phase diagram is qualitatively consistent with that of the lattice simulations [25, 29] except that ours have no confinement/deconfinement phase transition.

To look into chiral properties, we simultaneously depict the real part of VEV of Polyakov loop Φ and the constituent mass m_c as a function of L^{-1} with the bare mass fixed as $m = 0$ GeV and $m = 1$ GeV in Fig. 8. We here normalize the constituent mass as $m_c(L^1)/m_c(L^{-1} = 0)$. It is notable that chiral condensate, or equivalently, constituent quark mass does not undergo a clear transition even for large values of L^{-1}, and it gradually decreases. We thus have no clear chiral restoration transition while chiral symmetry is gradually restored in this theory. This result and the standard-PNJL result in [28] are consistent with those of the lattice simulation [29], which argues that the chiral restoration at weak coupling should occur at a quite small value of the compacted size L. The other notable point is that the chiral condensate undergoes quite small transitions coinciding with the deconfined/split and

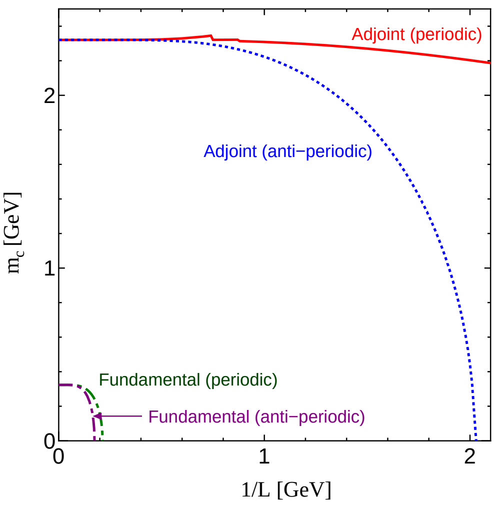

FIG. 6: Constituent mass m_c as a function of L^{-1} for $(N_f, N_a) = (2, 0)$ with aPBC, $(N_f, N_a) = (2, 0)$ with PBC, $(N_f, N_a) = (0, 2)$ with aPBC and $(N_f, N_a) = (2, 0)$ with PBC with the bare mass fixed as $m = 0$ GeV. We choose the parameter set as $\Lambda = 0.63$ GeV and $g_S \Lambda^2 = 2.19$ for fundamental cases and $\Lambda = 23.22$ GeV and $g_S \Lambda^2 = 0.63$ for adjoint cases.

split/re-confined phase transitions. (It can be seen better in Fig. 6 or the right panel for $m = 1$ GeV in Fig. 8.) This kind of the transition propagation is well studied in [74, 75], but they may be too small to be observed in the lattice simulations.

Let us briefly comment on non-perturbative deformation of the gluon potential discussed in Sec. II. We show one of the examples of the deformations in Eq. (A1) in Appendix. A, where introduction of the mass-dimension parameter M is not appropriate for the present purpose. Indeed, if we introduce this deformation ($M = 596$ MeV), the phase diagram in Fig. 4 is midified as Fig. 23. Here the confined phase emerges at small L^{-1} region, but it is connected with the re-confined phase through the small mass region. This result clearly shows that the gauge symmetry is broken as $SU(3) \to U(1) \times U(1)$ at zero-temperature or infinite-L. We note that the similar result with the same deformation in the gluon potential is shown in Ref. [28], where it is argued that the unified confined phase implies the volume-independece of the confined phase structure. This topic is beyond our scope, and we will not discuss it anymore.

We next consider $(N_f, N_a) = (1, 1)$ with PBC. We concentrate on the case with a massless fundamental quark, and the potential is given by $\mathcal{V}_g + \mathcal{V}_f^{\phi}(N_f = 1, m_f = 0) + \mathcal{V}_a^{\phi}(N_a = 1, m_a =$

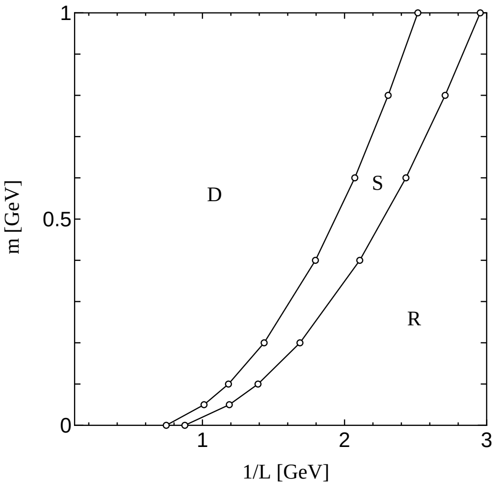

FIG. 7: L^{-1}-m phase diagram for $SU(3)$ gauge theory on $R^3 \times S^1$ with two-flavor PBC adjoint quarks $(N_f, N_a) = (0, 2)$ based on the PNJL-type effective potential. D stands for "deconfined", S for "split" and R for "re-confined" phases. Critical lines are first-order.

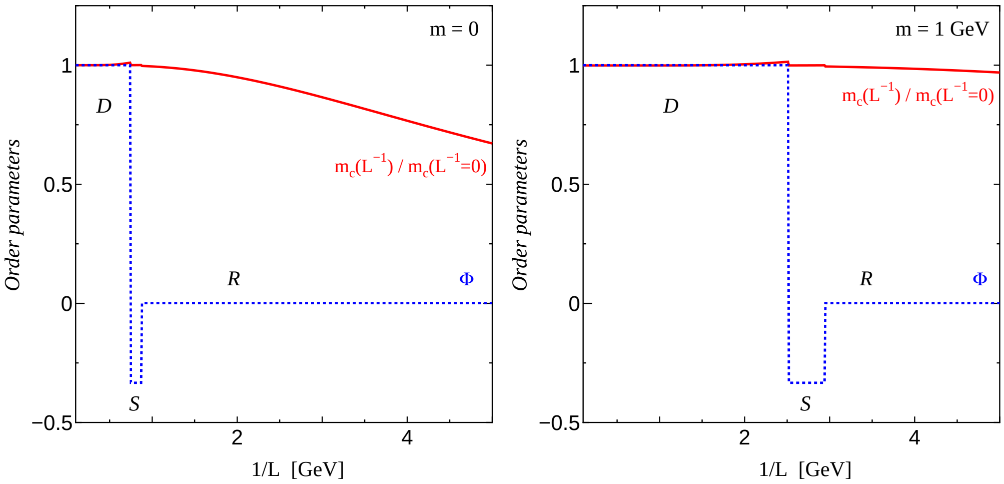

FIG. 8: VEV of Polyakov loop Φ (blue dashed) with $q_2 = 0$ and the constituent mass m_c (red solid) as a function of L^{-1} with the bare mass fixed as $m = 0$ GeV (left) and $m = 1$ GeV (right). The constituent mass is normalized as $m_c(L^{-1})/m_c(L^{-1} = 0)$. The result indicates that the chiral symmetry is gradually restored without the clear phase transition.

m). In this case, since the fundamental quark breaks the Z_3 center symmetry, the minima at $Re\Phi < 0$ become true vacua in the deconfined and split phases as shown in Fig. 9. (Fundamental matter with PBC moves the vacua to $Re\Phi < 0$ direction.) In addition, we have no exact re-confiend phase since $\Phi = 0$ vacuum cannot be chosen because of the center symmetry breaking in Fig. 9. We term this unusual phase as "pseudo-reconfined phase", where the $SU(3)$ is broken to $U(1) \times U(1)$ and Φ takes a nonzero and negative value. The existence of this phase is consistent with the research on flavor-number dependence of gauge-symmetry-broken manners in Ref. [8]. In Fig. 10, we depict the phase diagram for the same case. We emphasize that the split phase gets larger by introducing PBC fundamental quarks, compared to Fig. 4. It is because the center symmetry breaking chooses $(q_1, q_2, q_3) = (0, 0.5, 0.5)$ and its permutations as true vacua among all the possible minima Fig. 9, and makes it more stable than the center-symmetric case in Fig. 5.

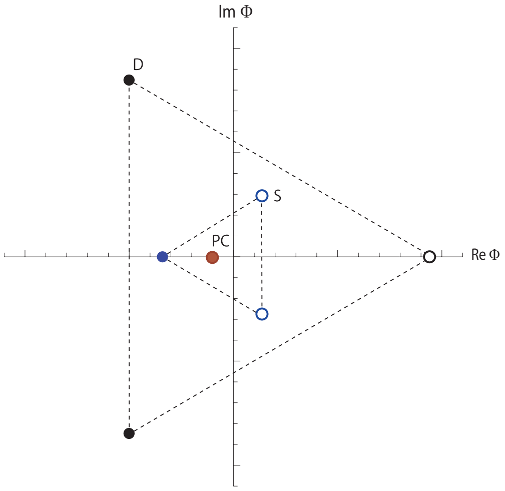

FIG. 9: Schematic distribution plot of Polyakov loop Φ for $SU(3)$ gauge theory on $R^3 \times S^1$ with one PBC adjoint and one PBC massless fundamental quarks $(N_f, N_a) = (1, 1)$. Points painted over stand for vacua in this case. Z_3 symmetry is broken, and some of the three minima are chosen as true vacua in deconfined and split phase. The Polyakov loop Φ in the pseudo-reconfined phase (PC) takes a nonzero and negative value.

To look into the details of pseudo-reconfined phase and the phase transition to the split phase, we depict the expanded effective potential near the global minima as a function of q_1 with $q_2 = 0$ in Fig. 11. The left panel shows the result for the massless adjoint quark ($m_a = m = 0$), which corresponds to the pseudo-confined phase. The minimum is not located at $(q_1, q_2) = (0.5, 0)$(split case) nor at $(q_1, q_2) = (1/3, 0)$(re-confined case). In the pseudo-confined phase we totally have six minima for q_1 and q_2 as $(q_1, q_2) \sim (0, 0.4)$, $(0.4, 0)$, $(-0.4, 0.4)$, $(-0.4, 0)$, $(0, -0.4)$, $(0.4, -0.4)$, which means that the vacua are given

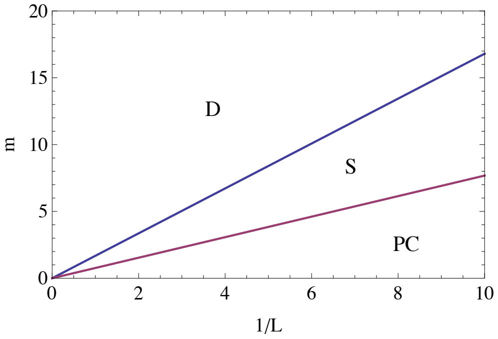

FIG. 10: Phase diagram for $R^3 \times S^1$ $SU(3)$ gauge theory with one PBC adjoint and one massless PBC fundamental quarks $(N_f, N_a) = (1, 1)$ based on the one-loop effective potential. m is the adjoint quark mass $m = m_a$ and L^{-1} is the inverse of the compacted size. PC stands for "pseudo-reconfined" phase.

by the permutation of $(q_1, q_2, q_3) \sim (0, 0.4, -0.4)$. The right panel shows the first-order phase transition between pseudo-confined and split phases. Since the potential barrier at the phase transition is quite low, the fluctuation could break down clear phase transition. For the cases with $(N_f, N_a) = (1, 2)$ and $(N_f, N_a) = (1, 3)$ where the flavor of adjoint quarks is larger than that of fundamental quarks, the minima of the potential in the pseudo-reconfined phase becomes deeper, and we can observe the first-order phase transition more distinctly.

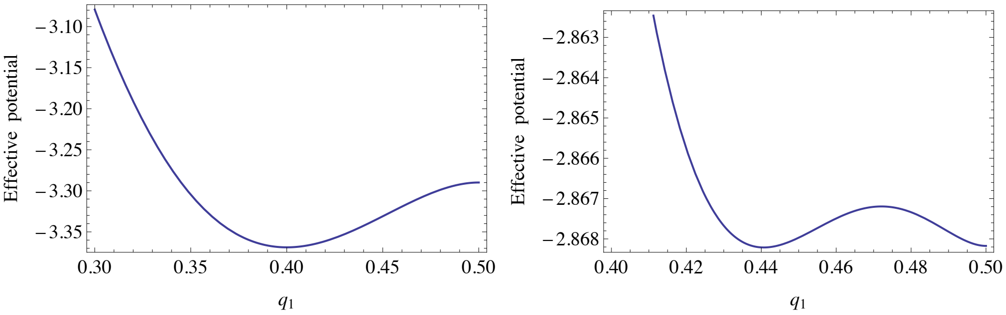

FIG. 11: Expanded effective potential of $R^3 \times S^1$ $SU(3)$ gauge theory with one PBC adjoint and one massless PBC fundamental quarks as a function of q_1 with $q_2 = 0$. Left one shows the case with the pseudo-reconfined phase ($m = m_a = 0$), where we have the minimum at $(q_1, q_2) \sim (0.4, 0)$. Right one shows the first-order phase transition between the pseudo-reconfined and split phase at $m_a L = 0.77$.

The chiral sector can be introduced by extending to $(N_f, N_a) = (2, 2)$. In this case we have two chiral sectors for fundamental and adjoint quarks, and we have arbitrariness how to implement four-point interactions and choose relative parameters. For example, we may consider the following forms of the four-point interactions.

$$
\begin{aligned}
&(g_S)_f[(\bar{\psi}_f\psi_f)^2+(\bar{\psi}_f i\gamma_5\vec{\tau}\psi_f)^2]+(g_S)_a[(\bar{\psi}_a\psi_a)^2+(\bar{\psi}_a i\gamma_5\vec{\tau}\psi_a)^2]\\
&\qquad+(g_S)_{fa}[\{(\bar{\psi}_f\psi_f)+(\bar{\psi}_f i\gamma_5\vec{\tau}\psi_f)\}\{(\bar{\psi}_a\psi_a)+(\bar{\psi}_a i\gamma_5\vec{\tau}\psi_a)\}],
\end{aligned}
\tag{20}
$$

where ψ_f and ψ_a stand for fundamental and adjoint quark fields, and $(g_S)_f, (g_S)_a, (g_S)_{fa}$ stand for fundamental, adjoint and mixing effective coupling. Even if we fix a form of the four-point interactions, we still have no criterion on how to set the parameters since there is no lattice study on this case either for aPBC or PBC. Thus we just comment on general aspects of the chiral properties in this case. For $(N_f, N_a) = (2, 0)$ with PBC, we know that we have the chiral phase transition as with that of aPBC as shown in Fig. 6. If this phase transition persists in the $(N_f, N_f) = (2, 2)$ case with PBC, chiral phase transition of the adjoint quarks could coincide with that of the fundamental chiral condensate [74, 75]. In such a scenario, the chiral phase diagram could be much richer than Fig. 8. However, whether this situation takes place depends on parameter sets $((g_S)_f, (g_S)_a, (g_S)_{fa})$, which can be fixed by using coming lattice data. We devote full investigation on this topic to future study.

Besides the cases we have shown above, we also have other interesting choices of matters. As shown in [76], the $SU(3)$ gauge theory with three fundamental flavors with flavored twisted boundary conditions $\phi = 0,\ 1/3,\ 2/3$ can accidentally keep the Z_3 center symmetry. For example, in the case of $(N_f, N_a) = (3, 1)$ with the flavored twisted boundary conditions $\phi = 0,\ 1/3,\ 2/3$ for fundamental fermions and PBC for the adjoint fermion, the distribution plot of Φ becomes symmetric as Fig. 5 and we have exact re-confined phase although the theory contains fundamental quarks. Moreover, in [77], the present authors and collaborators discuss the $SU(3)$ gauge theory with $(N_f, N_a) = (3, 0)$ with the flavored twisted boundary conditions $\phi = 0,\ 1/3,\ 2/3$ can lead to the spontaneous gauge symmetry breaking without adjoint quarks. This case is also fascinating as a future research topic.

IV. PHASE STRUCTURE IN FIVE DIMENSIONS

In this section, we discuss the vacuum and phase structure in $SU(3)$ gauge theories on $R^4 \times S^1$. Since the five-dimensional gauge theory is not renormalizable, we cannot discuss its non-perturbative aspects in a parallel way to the four-dimensional case. Thus we will concentrate on the one-loop part of the effective theory, and will not consider the contribution from the chiral sector. It is sufficient for our purpose of investigating the phase structure at weak-coupling.

We consider the five-dimensional one-loop effective potential $[\mathcal{V}_g + \mathcal{V}_f^0(N_f, m_f) + \mathcal{V}_a^0(N_a, m_a)]L^5$. We first look at the case with $(N_f, N_a) = (0, 1)$ with PBC. The qualitative properties are common with the four-dimensional case. Figure 12 shows the effective potential $[\mathcal{V}_g + \mathcal{V}_a^0(N_a = 1, m)]L^5$ as a function of q_1 with $q_2 = 0$ fixed. The adjoint quark mass is set as $mL = 0.5$, 1.3 and 2.0 from left to right panels. The three cases correspond to re-confined (left), split (center), and deconfined (right) phase. The contour plots at $mL = 0.5$(reconfined) and $mL = 1.3$(split) are depicted in Fig. 13. The manners of $SU(3)$ symmetry breaking and the distribution of Polyakov line Φ in each phase are the same as the four-dimensional case; $SU(3) \to U(1) \times U(1)$ in the re-confined phase and $SU(3) \to SU(2) \times U(1)$ in the split phase. We depict the phase diagram in L^{-1}-m for this case in Fig. 14. The qualitative configuration of the three phases in the phase diagram is indifferent from the four-dimensional case although the split phase is smaller in five dimensions.

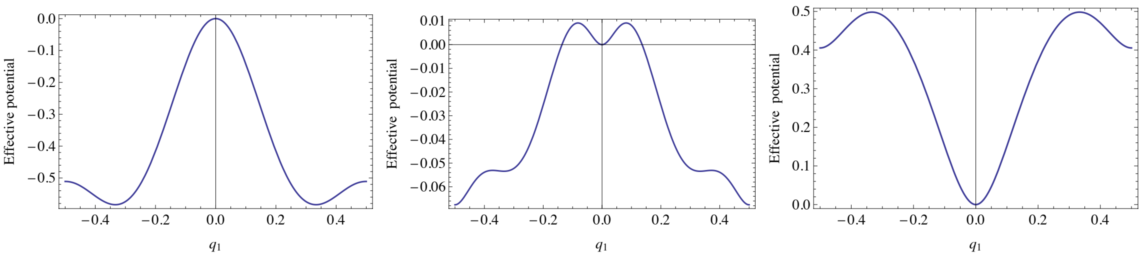

FIG. 12: The one-loop effective potential of $SU(3)$ gauge theory on $R^4 \times S^1$ with one PBC adjoint quark as a function of q_1 with $q_2 = 0$ $(\mathcal{V}_g + \mathcal{V}_a^0(1, m))L^5$. Depicted for $mL = 0.5$ (re-confined), 1.3 (split) and 2.0 (deconfined).

We next consider the case for $(N_f, N_a) = (1, 1)$ with PBC. We again concentrate on $m_f = 0$. Due to explicit breaking of Z_3 center symmetry, $\Phi < 0$ minima are chosen as

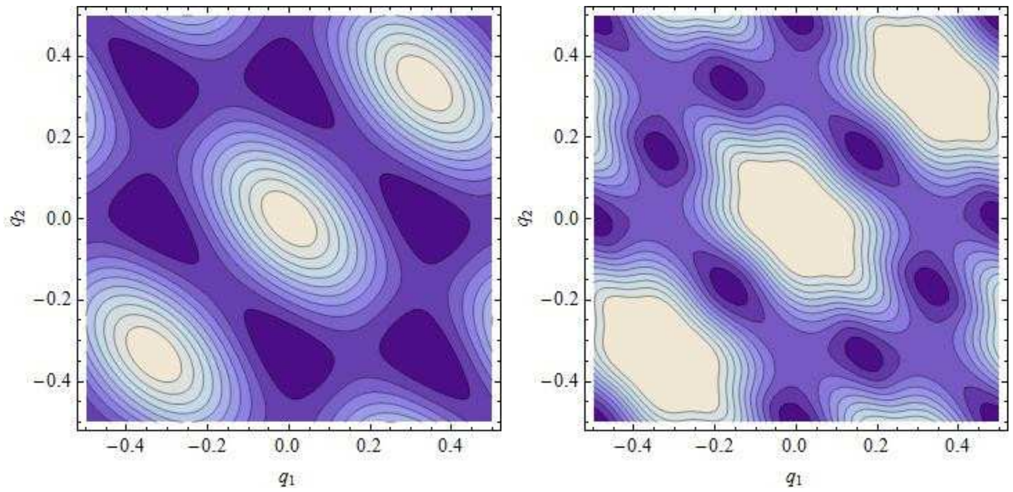

FIG. 13: Contour plot of the one-loop effective potential of $SU(3)$ gauge theory on $R^4 \times S^1$ with one PBC adjoint quark $(\mathcal{V}_g + \mathcal{V}_a^0(N_a = 1, m_a = m))L^5$ for $mL = 0.5$ and 1.3 as a function of q_1 and q_2.

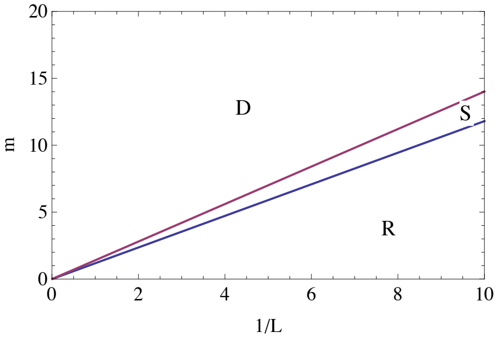

FIG. 14: L^{-1}-m_a phase diagram for $SU(3)$ gauge theory on $R^4 \times S^1$ with one PBC adjoint quark based on the one-loop effective potential.

vacua in the deconfined and split phases in the same way as the four dimensional case (Fig. 9). It is notable that the split phase is again enlarged by introducing fundamental fermions, but more effectively in five dimensions. Enhancement of the split phase due to the fundamental matter in five dimensions is sensitive to choice of parity pairs, or equivalently, choice of the number of flavors. For $(N_f, N_a) = (1, 1)$ without the parity pair, the pseudo-confined phase disappears and the split phase becomes the unique gauge-broken phase as shown in Fig. 15. This result is consistent with that of the massless case $(m_a = 0)$ in Ref. [9, 10]. On the other hand, when we introduce parity pairs for $(N_f, N_a) = (1, 1)$ or equivalently consider $(N_f, N_a) = (2, 2)$, the split phase becomes wider than that in Fig. 14 but the pseudo-reconfined phase still survives as shown in Fig. 16. In the five-dimensional pseudo-confined phase we again have six minima for q_1 and q_2 as $(q_1, q_2) \sim (0, 0.4)$, $(0.4, 0)$, $(-0.4, 0.4)$, $(-0.4, 0)$, $(0, -0.4)$, $(0.4, -0.4)$, which inidicates that the minima are given by the permutation of $(q_1, q_2, q_3) \sim (0, 0.4, -0.4)$. We depict the expanded effective potential in Fig. 17. The left panel shows the massless case ($m_a L = 0$), which corresponds to the pseudo-reconfined phase. The right panel shows the first-order phase transition between the pseudo-reconfined and split phases ($m_a L = 1.18$). In the cases with $(N_f, N_a) = (1, 2)$ or $(N_f, N_a) = (1, 3)$, the potential minima in the pseudo-reconfined phase becomes deeper and the phase transition gets more distinct.

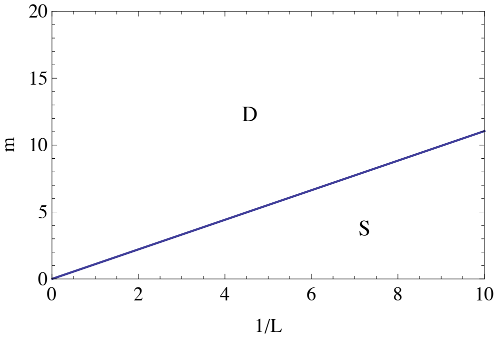

FIG. 15: L^{-1}-m_a phase diagram for $SU(3)$ gauge theory on $R^4 \times S^1$ with one adjoint and one massless fundamental quarks ($(N_f, N_a) = (1, 1)$, $m_f = 0$, PBC) based on the one-loop effective potential.

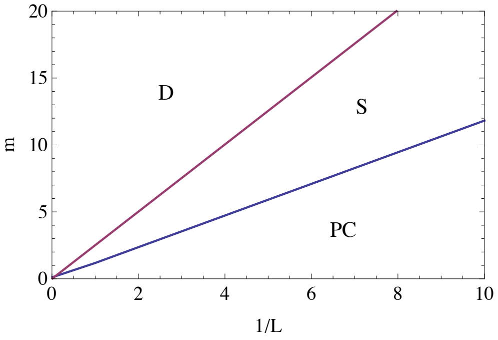

FIG. 16: L^{-1}-m_a phase diagram for $SU(3)$ gauge theory on $R^4 \times S^1$ with a set of parity pairs of $(N_f, N_a) = (1, 1)$, or equivalently $(N_f, N_a) = (2, 2)$, based on the one-loop effective potential.

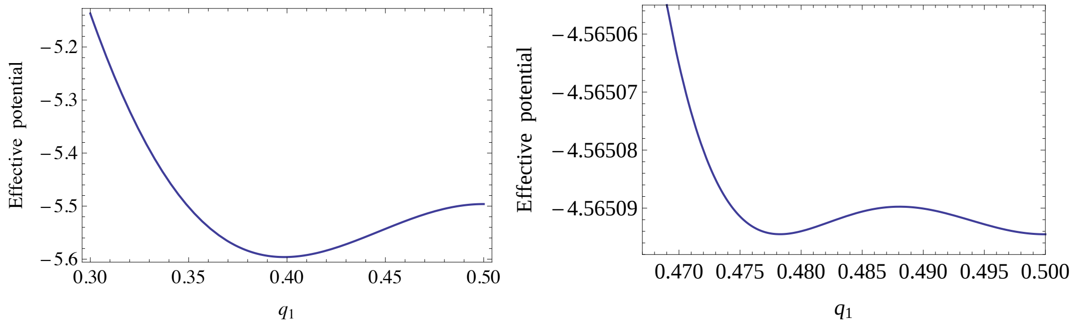

FIG. 17: Expanded 5D effective potential of $SU(3)$ gauge theory on $R^4 \times S^1$ with a set of parity pairs of $(N_f, N_a) = (1,1)$ or $(N_f, N_a) = (2,2)$ as a function of q_1 with $q_2 = 0$. Left one shows the pseudo-confined phase ($m = m_a = 0$), where we have the minimum at $(q_1, q_2) \sim (0.4, 0)$. Right one shows the first-order phase transition between the pseudo-reconfined and split phase at $m_a L = 1.18$.

In the end of this section we comment on the other aspect of gauge theory with a compacted dimension. If we regard the compacted direction as time direction, the boundary condition for the Polyakov-loop phases can be seen as imaginary chemical potential. The periodic and anti-periodic boundary conditions correspond to different Roberge-Weiss transition points on the QCD phase diagram. From this viewpoint, it is clear that fundamental fermions with PBC works to move the vacua to $\mathrm{R}e\Phi < 0$ direction as shown in Fig. 9 while those with aPBC move it to $\mathrm{R}e\Phi > 0$ direction as shown in Fig. 18

V. SUMMARY

In this paper we have studied the phase diagram for $SU(3)$ gauge theories with a compact spatial dimension by using the effective models, with emphasis on the dynamical gauge symmetry breaking. We show that introduction of adjoint matter with periodic boundary condition leads to the unusual phases with spontaneous gauge symmetry breaking, whose ranges are controlled by intorducing fundamental matter. We also study chiral properties in these theories and show that the chiral condensate remains nonzero even at a small compacted size.

In Sec. II, we developed our setup based on one-loop effective potential and four-point fermion interactions. The effective potential is composed of the gluon, quark and chiral

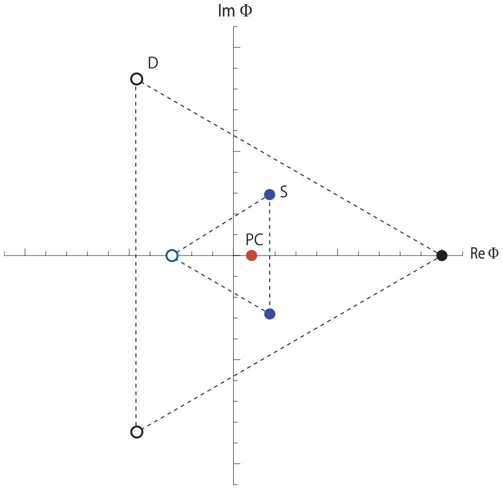

FIG. 18: Schematic distribution plot of Polyakov loop Φ for SU(3) gauge theory with one PBC adjoint and one aPBC fundamental quarks. Points painted over stand for vacua in this case. Z_3 symmetry is broken in the different manner from Fig. 9.

sectors. The total effective potential corresponds to that of the PNJL model with one-loop gluon potential. This setup is effective enough to investigate vacuum structure and chiral properties at weak-coupling or small size of the compact dimension.

In Sec. III, we elucidated the vacuum and phase structure in $SU(3)$ gauge theory on $R^3 \times S^1$. The theory with PBC adjoint quarks has three different phases in the L^{-1}-m space, including the deconfined phase ($SU(3)$, nonzero Φ), the split phase ($SU(2) \times U(1)$, nonzero Φ) and the re-confined phase ($U(1) \times U(1)$, zero Φ with nontrivial global minima). The configuration of these phases in the phase diagram is consistent with that of the lattice calculations although we have no confined phase. By using the PNJL effective potential, we argued that chiral symmetry is slowly restored without clear phase transition when the size of the compact dimension is decreased. In this section we also studied vacuum and phase structure for the case with both fundamental and adjoint matters, and showed that the split phase is generically widened by adding PBC fundamental quarks. We consider that it is because one of the three possible minima for the split phase becomes more stable due to the center symmetry breaking. We showed that another $U(1) \times U(1)$ phase with a negative value of Φ emerges in this case (pseudo-reconfined phase).

In Sec. IV, we studied the vacuum and phase structure in $SU(3)$ gauge theory on $R^4 \times S^1$. In the five-dimensional case we concentrate on the one-loop part of the effective potential.

The theory with PBC adjoint quarks again has the split ($SU(2) \times U(1)$) and re-confined ($U(1) \times U(1)$) phases. Introduction of fundamental quarks works to enlarge the split phase more effectively than the four-dimensional case. Especially in the case with one adjoint and one fundamental quarks without parity pairs, the split phase overcomes the pseudo-reconfined phase and becomes a unique gauge-symmetry-broken phase.

In the end of the paper, we discuss whether the lattice simulation can check our predictions. One of our main results is that enlargement of the split phase in the presence of fundamental fermions. This property would be observed in the on-going lattice simulations on four-dimesional gauge theory with a compact direction [78]. The pseudo-reconfined phase can be also observed where the VEV of Polyakov loop becomes negative but different from that of the split phase. On the other hand, it seems difficult to show the first-order phase transition between the pseudo-reconfined and split phases. The lattice calculation can check whether chiral condensate remains finite in the re-confined phase even at a very small compacted size. The small chiral transitions coinciding with the gauge-symmetry phase transitions are subtle. If the lattice simulation succeeds to measure chiral susceptibility with high precision, this phenomena may be able to be observed.

During preparing this draft, the collaboration [78] kindly informed us that it also performed perturbative calculations on the phase diagram in gauge theory on $R^3 \times S^1$ and $R^4 \times S^1$. It could be valuable for readers to compare the results from the two independent groups.

Acknowledgments

The authors are grateful to E. Itou for giving them chances to have interest in the present topics and reading the draft carefully. They are thankful to Y. Hosotani, H. Hatanaka and H. Kouno for their careful reading of this manuscript and valuable comments. They also thank G. Cossu and J. Noaki for the kind co-operation. K. K. thanks H. Nishimura for useful comments. K.K. is supported by RIKEN Special Postdoctoral Researchers Program. T.M. is supported by Grand-in-Aid for the Japan Society for Promotion of Science (JSPS) Postdoctoral Fellows for Research Abroad(No.24-8).

Appendix A: Vacua and phase structures for other cases

1. Gauge symmetric cases

In this appendix, we discuss the vacuum structure for the several gauge-symmetric cases in $R^3 \times S^1$ $SU(3)$ gauge theory. We concentrate on massless cases as $m_a = m_f = 0$. The potential contour plot for $(N_f, N_a) = (0,0)$ (pure gauge theory) is shown in Fig. 19. The effective potential has the minima at $(q_1, q_2) = (0,0)$, $(1/3, 1/3)$, $(-1/3, -1/3)$. Since it means that the three Polyakov-line phases are equivalent in the vacuum ($q_1 = q_2 = q_3$), the $SU(3)$ gauge symmetry is intact.

The case with one fundamental fermion with anti-periodic boundary condition is shown in Fig. 20. The fundamental quark breaks Z_3 symmetry explicitly and thus, two of the three minima become the meta-stable. If the boundary condition of fermion is changed to the periodic one, the global minima move to $(\pm 1/3, \pm 1/3)$ as shown in Fig. 21. On the other hand, the case for an adjoint fermion with anti-periodic boundary condition is similar to the pure gauge case as shown in Fig. 22 since it keeps the Z_3 center symmetry.

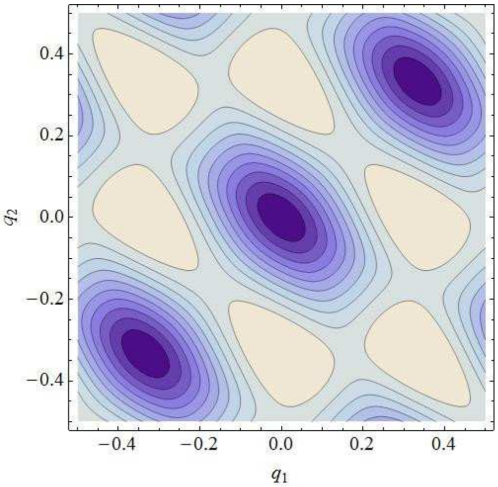

FIG. 19: The contour plot of one-loop effective potential for pure $SU(3)$ gauge theory, $\mathcal{V}_g L^4$ as a function of q_1 and q_2. Thicker region stands for deeper region of the effective potential.

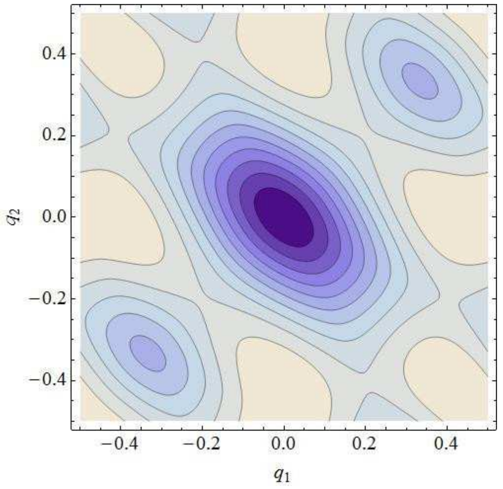

FIG. 20: The contour plot of one-loop effective potential for $R^3 \times S^1$ $SU(3)$ gauge theory with one massless fundamental fermion with anti-periodic boundary condition ($(N_f, N_a) = (1, 0)$ with aPBC) $(\mathcal{V}_g + \mathcal{V}_f^{1/2})L^4$.

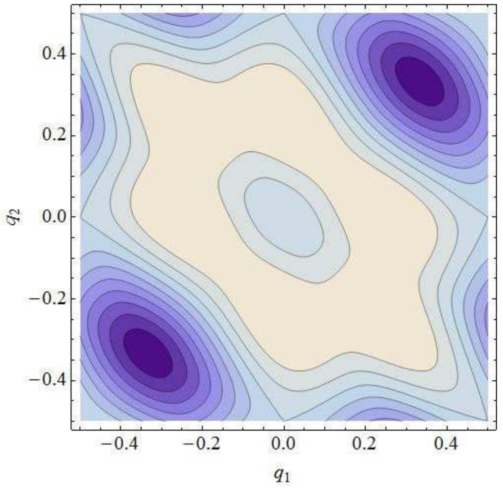

FIG. 21: The contour plot of one-loop effective potential for $R^3 \times S^1$ $SU(3)$ gauge theory with one fundamental fermion with periodic boundary condition ($(N_f, N_a) = (1, 0)$ with PBC) $(\mathcal{V}_g + \mathcal{V}_f^0)L^4$.

2. Phase diagram with non-perturbative deformation

In Fig. 23, we depict the phase diagram for $R^3 \times S^1$ $SU(3)$ gauge theory with $(N_f, N_a) = (0, 1)$ with PBC based on the nonperturbatively deformed gluonic potential. As an example,

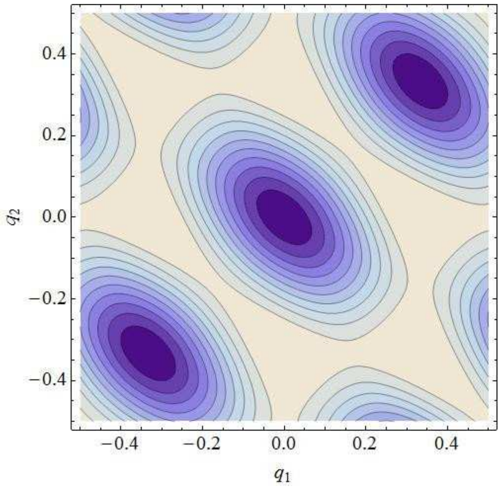

FIG. 22: The contour plot of one-loop effective potential for $R^3 \times S^1$ $SU(3)$ gauge theory with the $N_a = 1$ adjoint fermion with anti-periodic boundary condition ($(N_f, N_a) = (0, 1)$ with aPBC) $(\mathcal{V}_g + \mathcal{V}_a^{1/2})L^4$.

we consider the following modification from the perturbative potential in [27, 28, 69, 70]:

$$\mathcal{V}_g^{\rm np} = -\frac{2}{L^4\pi^2}\sum_{i,j=1}^{N}\sum_{n=1}^{\infty}\Big(1-\frac{1}{N}\delta_{ij}\Big)\frac{\cos(2n\pi q^{ij})}{n^4} + \frac{M^2}{2\pi^2 L^2}\sum_{i,j=1}^{N}\sum_{n=1}^{\infty}\Big(1-\frac{1}{N}\delta_{ij}\Big)\frac{\cos(2n\pi q^{ij})}{n^2} \tag{A1}$$

where M is the mass-dimension 1 parameter. We set the scale parameter as $M = 596$ MeV. The confined phase and the first-order phase transition show up, but it is merged into the gauge-broken re-confined phase. We note that the $SU(3)$ gauge symmetry is explicitly broken in the confined (re-confined) phase.

---

[1] ATLAS Collaboration, Phys. Lett. B **716** (2012) 1.

[2] CMS Collaboration, Phys. Lett. B **716** (2012) 30.

[3] N. Manton, Nucl.Phys.B **158** (1979) 141.

[4] Y. Hosotani, Phys.Lett.B **126**, 309 (1983).

[5] Y. Hosotani, Annals Phys **190**, 233 (1989).

[6] A. T. Davies and A. McLachlan, Phys. Lett. B **200** (1988) 305; Nucl. Phys. B **317** (1989) 237.

[7] H. Hatanaka, T. Inami and C. S. Lim, Mod. Phys. Lett. A **13** (1998) 2601.

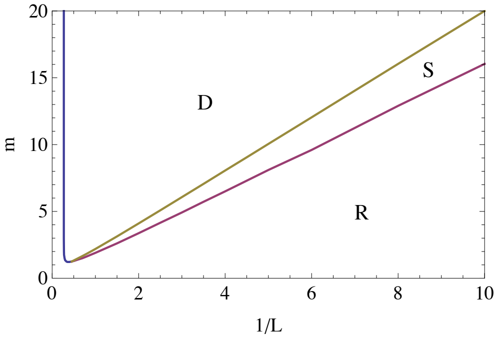

FIG. 23: Phase diagram for $R^3 \times S^1$ SU(3) theory with one PBC adjoint quark based on the effective potential with non-perturbative deformation ($M = 596$ MeV). C stands for “confined”, D stands for “deconfined” and S for “split” phases. Compared to the perturbative one-loop case, the confined phase emerges but merges into the re-confined phase.

[8] H. Hatanaka, Prog. Theor. Phys. **102** (1999) 407 [arXiv:hep-th/9905100].

[9] Y. Hosotani, Proceedings for DSB 2004, Nagoya (2005) [arXiv:hep-ph/0504272].

[10] Y. Hosotani, Proceedings for GUT 2012, Kyoto (2012) [arXiv:1206.0552].

[11] K. Agashe, R. Contino and A. Pomarol, Nucl. Phys. B **719** (2005) 165.

[12] N. Maru, K. Takenaga, Phys.Lett.B **637**, 287 (2006) [arXiv:hep-ph/0602149].

[13] Y. Hosotani, N. Maru, K. Takenaga and T. Yamashita, Prog. Theor. Phys. **118** (2007) 1053 [arXiv:0709.2844].

[14] M. Sakamoto, K. Takenaga, Phys.Rev.D **76**, 085016 (2007) [axXiv:0706.0071].

[15] Y. Hosotani, K. Oda, T. Ohnuma and Y. Sakamura, Phys. Rev. D**78** (2008) 096002; **79** (2009) 079902.

[16] M. Sakamoto and K. Takenaga, Phys. Rev. D **80** (2009) 085016 [arXiv:0908.0987].

[17] Y. Hosotani, P. Ko and M. Tanaka, Phys. Lett. B **680** (2009) 179.

[18] K. Ishiyama, M. Murata, H. So and K. Takenaga, Prog. Theor. Phys. **123** (2010) 257 [arXiv:0911.4555]

[19] Y. Hosotani, S. Noda and N. Uekusa, Prog. Theor. Phys. **123** (2010) 757.

[20] Y. Hosotani, M. Tanaka and N. Uekusa, Phys. Rev. D **82** (2011) 115024.

[21] Y. Hosotani, M. Tanaka and N. Uekusa, Phys. Rev. D **84** (2011) 075014.

[22] H. Hatanaka and Y. Hosotani, Phys. Lett. B **713** (2012) 481.

[23] N. Irges and F. Knechtli, K. Yoneyama, [arXiv:1212.5514].

[24] M. C. Ogilvie, [arXiv:1211.2843].

[25] J. C. Myers, M. C. Ogilvie, Phys.Rev.D **77**, 125030 (2008) [arXiv:0707.1869].

[26] J. C. Myers, M. C. Ogilvie, PoS Lattice2008, 201 (2008) [arXiv:0809.3964].

[27] J. C. Myers, M. C. Ogilvie, JHEP **07(2012)**, 095 (2009) [arXiv:0903.4638].

[28] H. Nishimura, M. C. Ogilvie, Phys.Rev.D **81**, 014018 (2010) [arXiv:0911.2696].

[29] G. Cossu, M. D'Elia, JHEP **07(2009)**, 048 (2009) [arXiv:0904.1353].

[30] M. Creutz, Phys.Rev.Lett **43**, 553 (1979).

[31] H. Kawai, M. Nio and Y. Okamoto, Prog. Theor. Phys. **88** (1992) 341.

[32] J. Nishimura, Mod. Phys. Lett. A **11** (1996) 3049 [arXiv:hep-lat/9608119].

[33] B. B. Beard et al., Nucl. Phys. Proc. Suppl. **63** (1998) 775 [arXiv:hep-lat/9709120].

[34] C. B. Lang, M. Pilch and B. S. Skagerstam, Int. J. Mod. Phys. A **3** (1988) 1423.

[35] S. Chandrasekharan and U. J. Wiese, Nucl. Phys. B **492** (1997) 455 [arXiv:hep-lat/9609042].

[36] R. Brower, S. Chandrasekharan and U. J. Wiese, Phys. Rev. D **60** (1999) 094502 [arXiv:hep-th/9704106].

[37] S. Ejiri, J. Kubo and M. Murata, Phys. Rev. D **62** (2000) 105025 [arXiv:hep-ph/0006217].

[38] S. Ejiri, S. Fujimoto and J. Kubo, Phys. Rev. D **66** (2002) 036002 [arXiv:hep-lat/0204022].

[39] P. Dimopoulos, K. Farakos, A. Kehagias and G. Koutsoumbas, Nucl. Phys. B **617** (2001) 237 [arXiv:hep-th/0007079].

[40] P. Dimopoulos, K. Farakos, C. P. Korthals-Altes, G. Koutsoumbas and S. Nicolis, JHEP **02(2001)** 005 [arXiv:hep-lat/0012028].

[41] P. Dimopoulos, K. Farakos and G. Koutsoumbas, Phys. Rev. D **65** (2002) 074505 [arXiv:hep-lat/0111047].

[42] K. Farakos, P. de Forcrand, C. P. Korthals Altes, M. Laine and M. Vettorazzo, Nucl. Phys. B 655 (2003) 170 [arXiv:hep-ph/0207343].

[43] N. Irges and F. Knechtli, Nucl. Phys. B **719** (2005) 121 [arXiv:hep-lat/0411018].

[44] N. Irges and F. Knechtli, hep-lat/0604006.

[45] N. Irges and F. Knechtli, Nucl. Phys. B **775** (2007) 283 [arXiv:hep-lat/0609045].

[46] N. Irges, F. Knechtli and M. Luz, JHEP **08(2007)** 028 [arXiv:0706.3806].

[47] F. Knechtli, N. Irges, M. Luz, J.Phys.Conf.Ser. **110**,102006 (2008) [arXiv:0711.2931].

[48] N. Irges and F. Knechtli, Nucl. Phys. B **822** (2009) 1 [arXiv:0905.2757].

[49] N. Irges and F. Knechtli, Phys. Lett. B **685** (2010) 86 [arXiv:0910.5427].

[50] L. Del Debbio, E. Kerrane and R. Russo, Phys. Rev. D **80** (2009) 025003 [arXiv:0812.3129].

[51] P. de Forcrand, A. Kurkela, M. Panero, JHEP **06(2010)**, 050 (2010) [arXiv:1003.4643].

[52] L. Del Debbio, A. Hart, E. Rinaldi, JHEP **07(2012)** 178 [arXiv:1203:2116].

[53] N. Irges and F. Knechtli, K. Yoneyama, Nucl.Phys.B **865** (2012) 541 [arXiv:1206.4907].

[54] A. Gocksch and M. Ogilvie, Phys. Rev. D31, 877 (1985).

[55] K. Fukushima, Phys. Lett. B591, 277 (2004), [arXiv:hep-ph/0310121].

[56] S. P. Klevansky, Rev. Mod. Phys. 64, 649 (1992).

[57] T. Hatsuda and T. Kunihiro, Phys. Rept. 247, 221 (1994), [arXiv:hep-ph/9401310].

[58] C. Ratti, S Roessner, M. A. Thaler, W. Weise, Eur.Phys.J.C **49**, 213 (2007) [arXiv:hep-ph/0609218].

[59] T. Eguchi and H. Kawai, Phys. Rev. Lett. 48, 1063 (1982).

[60] P. Kovtun, M. Unsal, L. G. Yaffe, JHEP **06(2007)**, 019 (2007), [arXiv:hep-th/0702021].

[61] M. Unsal, Phys. Rev. Lett. **100**, 032005 (2008) [arXiv:0708.1772].

[62] M. Unsal and L. G. Yaffe, Phys. Rev. D **78**, 065035 (2008) [arXiv:0803.0344].

[63] B. Bringoltz and S. R. Sharpe, Phys. Rev. D**78**, 034507 (2008) [arXiv:0805.2146].

[64] B. Bringoltz, JHEP **06(2009)**, 091 (2009) [arXiv:0905.2406].

[65] B. Bringoltz and S. R. Sharpe, Phys. Rev. D **80**, 065031 (2009) [arXiv:0906.3538].

[66] E. Poppitz and M. Unsal (2009), JHEP **01(2010)**, 098 (2010) [arXiv:0911.0358].

[67] D. Gross, R. Pisarski, L. Yaffe, Rev.Mod.Phys **53**, 43 (1981).

[68] N. Weiss, Phys.Rev.D **24**, 475 (1981).

[69] P. N. Meisinger, T. R. Miller, and M. C. Ogilvie, Phys. Rev. D **65**, 034009 (2002) [arXiv:hep-ph/0108009].

[70] P. N. Meisinger and M. C. Ogilvie, Phys.Rev.D **81**, 025012 (2010) [arXiv:0905.3577].

[71] A. Dumitru, et.al., Phys.Rev.D **83**, 034022 (2011) [arXiv:1011.3820]; A. Dumitru, et.al., Phys.Rev.D **86**, 105017 (2012) [arXiv:1205.0137].

[72] F. Karsch and M. Lutgemeier, Nucl. Phys. B **550**, 449 (1999) [arXiv:hep-lat/9812023].

[73] J. Engels, S. Holtmann and T. Schulze, Nucl. Phys. B **724**, 357 (2005) [arXiv:hep-lat/0505008].

[74] A. Barducci, R. Casalbuoni, G. Pettini, R. Gatto, Phys.Lett.B **301**, 95 (1993).

[75] K. Kashiwa, Y. Sakai, H. Kouno, M. Matsuzaki, M. Yahiro, J.Phys.G **36**, 105001 (2009) [arXiv:0804.3557].

[76] H. Kouno, Y. Sakai, T. Makiyama, K. Tokunaga, T. Sasaki, M. Yahiro, J.Phys.G **39** (2012)

085010-1 085010-21; Y. Sakai, H. Kouno, T. Sasaki and M. Yahiro, Phys.Lett.B **718** (2012) 130.

[77] H. Kouno, K. Kashiwa, T. Misumi, T. Makiyama, T Sasaki, M. Yahiro, in preparation.

[78] G. Cossu, H. Hatanaka, Y. Hosotani, E. Itou, J. Noaki, work in progress.

[79] One may ask whether $N_a = 2$ corresponds to the conformal window. However, since we introduce nonzero quark mass in our study, the conformality, even if exists, is broken.